Inorganic Chemistry

ARTICLE

pubs.acs.org/IC

DNA Cleavage Activity of Fe(II)N4Py under Photo Irradiation in the Presence of 1,8-Naphthalimide and 9-Aminoacridine: Unexpected Effects of Reactive Oxygen Species Scavengers

Qian Li, Wesley R. Browne,* and Gerard Roelfes*

Stratingh Institute for Chemistry, University of Groningen, Nijenborgh 4, 9747 AG, Groningen, The Netherlands

Supporting Information

ABSTRACT:

The DNA cleavage activity of the iron(II) complex of the ligand *N*,*N*-bis(2-pyridylmethyl)-*N*-bis(2-pyridyl)methylamine (N4Py) was investigated in the presence of the chromophores 1,8-naphthalimide (NI) and 9-aminoacridine (AA) under photo irradiation at 355 and 400.8 nm and compared to the activity of the complex without the chromophores. Whereas in most cases no synergistic effect of the added chromophores on DNA cleavage efficiency was observed, it was found that for Fe(II)N4Py, in combination with NI under irradiation at 355 nm, the DNA cleavage activity was increased. Surprisingly, it was found that the addition of reactive oxygen species (ROS) scavengers gave rise to significantly increased DNA cleavage efficiency, which is a highly counterintuitive observation since ROS are needed to achieve DNA cleavage. A hypothesis is put forward to explain, at least partly, these results. It is proposed that the addition of scavengers inhibits quenching of ^{3}NI*, thus making photo-induced electron transfer between ^{3}NI* and Fe(III)N4Py more efficient. This results in reduction of Fe(III)N4Py to Fe(II)N4Py, which can then react with ROS giving rise to DNA cleavage. Hence the role of the scavengers is to maintain a close to optimal concentration of ROS. The present study serves as an illustration of the care that needs to be exercised in interpreting the results of experiments using standard ROS scavengers, since especially in complex systems such as presented here they can give rise to unexpected phenomena. In the presence of 1,8-naphthalimide or 9-aminoacridine, ROS scavengers can increase the DNA cleavage efficiency of Fe(II)N4Py complex under photo irradiation.

INTRODUCTION

The pentadentate ligand *N*,*N*-bis(2-pyridylmethyl)-*N*-bis(2-pyridyl)-methylamine (N4Py, Chart 1) was designed and synthesized as a mimic of the metal-binding domain of the bleomycins (BLMs), a family of natural antibiotics clinically used in the treatment of certain cancers, e.g., cancers of the cervix, head, neck, and testicles.[1−4] As both a structural and functional model of Fe(II)-BLM, the Fe(II)N4Py complex is capable of inducing DNA strand breaks efficiently with molecular oxygen as the terminal oxidant, even in the absence of an external reducing agent.[5] A structural analogue of 'activated BLM', i.e., the N4Py-Fe(III)-OOH intermediate, has been proposed as the active species or precursor in DNA cleavage.[5f]

We recently reported that the DNA cleavage activity of Fe(II)N4Py complexes is increased substantially by photo irradiation, which is dependent on the structural characteristics of the complexes and the wavelength and intensity of irradiation.[5g] Mechanistic investigations have revealed that the reactive oxygen species (ROS) $O_2^{\bullet-}$, $^1O_2$, and $HO^{\bullet}$ contribute to the photo-enhanced DNA cleavage activity and that their relative contribution is dependent on the irradiation wavelength.[5g] The origin of the increase in activity is proposed to be mainly the photo-enhanced formation of N4Py-Fe(III)-OOH.[5g]

The DNA binding moieties introduced to the N4Py ligand covalently in our previous study, i.e., 1,8-naphthalimide (NI) and 9-aminoacridine (AA) (Chart 1), are well-known photo sensitizers capable of DNA photo cleavage, in which photo-induced

Received: April 22, 2011
Published: July 22, 2011

Chart 1. N4Py, NI, and AA

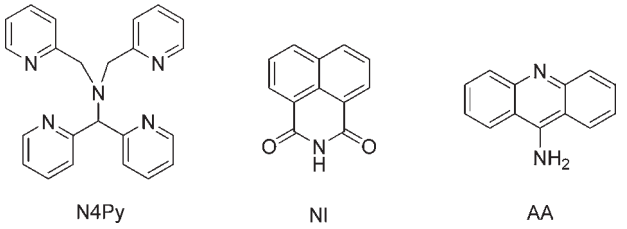

electron transfer (PET) plays a key role.[6] The presence of these chromophores could further enhance the DNA cleavage activity of Fe(II)N4Py under photo irradiation, by PET. Furthermore, the activity of Fe(II)N4Py could be selectively sensitized by NI and AA at various wavelengths due to the differences in their UV−vis absorption spectra. We report here on the effect of the presence of NI and AA on the DNA cleavage activity of Fe(II)N4Py under photo irradiation in aerobic conditions, in the absence of reducing agents. The mechanism of the DNA cleavage process was investigated by employing a series of reactive oxygen species (ROS) scavengers as mechanistic probes, which resulted, unexpectedly, in enhancement of DNA cleavage activity.

EXPERIMENTAL SECTION

Materials and Instrumentation. All reagents and solvents were used as purchased without further purification unless noted otherwise. NI and AA were purchased from Sigma-Aldrich and purified by crystallization from MeOH and Et_2O. $[Fe(II)(N4Py)(CH_3CN)](ClO_4)_2 \cdot 2H_2O$ was synthesized according to literature procedures, and all data are in agreement with those reported.[5a] UV−vis absorption spectra were recorded using 1, 5, or 10 cm path length quartz cells on a JASCO V-660 spectrophotometer. Absorption maxima are ±2 nm, and molar absorptivities are ±5%. All spectra were recorded at 20 °C. Photo irradiation was performed by using continuous wave (CW) lasers (400.8 nm, 50 mW at source, PowerTechnology; 355 nm, 10 mW at source, Cobolt). The power at the sample was determined using the quantum counter ferrioxalate and verified using a power sensor (PM10 V1, with a FieldMate Laser Power Meter, Coherent).

pUC18 plasmid DNA, isolated from *Escherichia coli* XL-1-blue, was purified using QIAGEN maxi kits. Concentrations were determined by the absorption at 260 nm using a NanoDrop 1000 spectrophotometer (Thermo Scientific). Restriction enzymes and restriction buffers were purchased from New England Biolabs (NEB). DNA ladder (SmartLadder, 0.2−10 kbp) was purchased from Eurogentec. Catalase (from bovine liver) and superoxide dismutase (SOD, from bovine erythrocytes) were purchased from Sigma-Aldrich. Agarose used for the gel electrophoreses was purchased from Invitrogen. Pictures of the gel slabs were taken with a Spot Insight CCD camera using the software program Spot version 3.4. The intensity of the bands on the film was quantified by using the software program Gel-Pro Analyzer version 4.0. Statistical calculations were performed using Mathematica version 7.01.

Determination of Irradiation Power. The iron(III) oxalate/phenanthroline actinometer system was used to determine the light flux (R) of irradiation.[7] The power (P) at the sample was calculated using eq 1, in which E_p is the energy of one photon, $\hbar$ is Planks constant (6.626×10^{-34} Js), c is the speed of light (3.0×10^8 ms^{-1}), and λ is the wavelength of light source (355 and 400.8 nm). The values of power determined by actinometry are in a good agreement with that measured by using the power sensor. Detailed information of the actinometry is provided as Supporting Information.

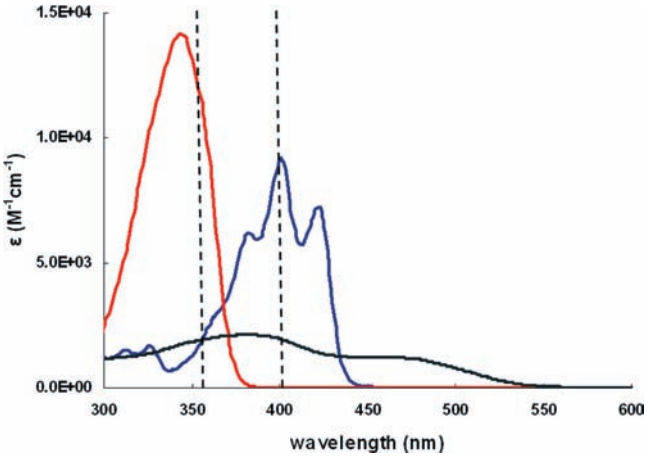

Figure 1. UV−vis absorption spectra of NI (red line), AA (blue line), and Fe(II)N4Py (black line).

$$P = E_p R = \frac{\hbar c}{\lambda} R \quad (1)$$

DNA Cleavage Experiments. $[Fe(II)(N4Py)(CH_3CN)](ClO_4)_2 \cdot 2H_2O$ was dissolved in H_2O, and 0.5% v/v DMF was used to aid the dissolution of NI and AA in H_2O. The respective solutions were added to a buffered solution (10 mM of Tris-HCl, pH of 8.0) of supercoiled pUC18 plasmid DNA in 1.5 mL of eppendorfs. (The final concentration of DMF in the reaction solution was <0.05%.) The reaction solutions, with a final volume of 50 μL and a final concentration of 1.0 μM iron(II) complex and 0.1 μg μL^{-1} DNA (150 μM in base pairs), with or without 1.0 or 5.0 μM NI and AA, were incubated at 37 °C in the dark under laser irradiation at 400.8 or 355 nm. For comparison, experiments were performed under ambient lighting, which gave the same results as experiments performed in the dark (data not shown).

Samples (2 μL) were taken from the reaction solutions after 30 min and quenched by addition to 15 μL of a NaCN solution (1 mg mL^{-1}, containing 2040 equiv of NaCN with respect to Fe(II)N4Py) with 3 μL of loading buffer (consisting of 0.08% bromophenol blue and 40% sucrose, 6 × conc.) and immediately frozen in liquid nitrogen. The samples were run on 1.2% agarose gels in 1 × Tris-acetate-EDTA (TAE) buffer for at least 90 min at 70 V. Gels were stained in an ethidium bromide (EtBr) bath (1.0 μg mL^{-1}) for 45 min and then washed with gel running buffer. Quantification was performed by fluorescence imaging, and a correction factor of 1.31 was used to compensate for the reduced EtBr uptake capacity of supercoiled plasmid pUC18 DNA.[5d] All data are the average of cleavage experiments that were performed at least in triplicate.

Quantification of *ssc* and *dsc*. The average number of single- (n) and double-strand cuts (m) in a DNA molecule was calculated using both eqs 2 and 3, in which f_{III} and f_I is the fraction of linear DNA and supercoiled DNA, respectively.[8] Equation 4 is the Freifelder−Trumbo relationship,[9] in which h is the maximum distance in base pairs between nicks on opposite strands to generate a double strand cut (i.e., 16), and L is the total number of base pairs of the DNA used (2686 bp for pUC18 plasmid DNA). Uncertainties in the values of m and n were calculated by a Monte Carlo simulation as described previously.[5d]

$$f_{III} = m \times e^{-m} \quad (2)$$

$$f_I = e^{-(m+n)} \quad (3)$$

$$m = \frac{n^2(2h+1)}{4L} \quad (4)$$

dx.doi.org/10.1021/ic2008478 |*Inorg. Chem.* 2011, 50, 8318–8325

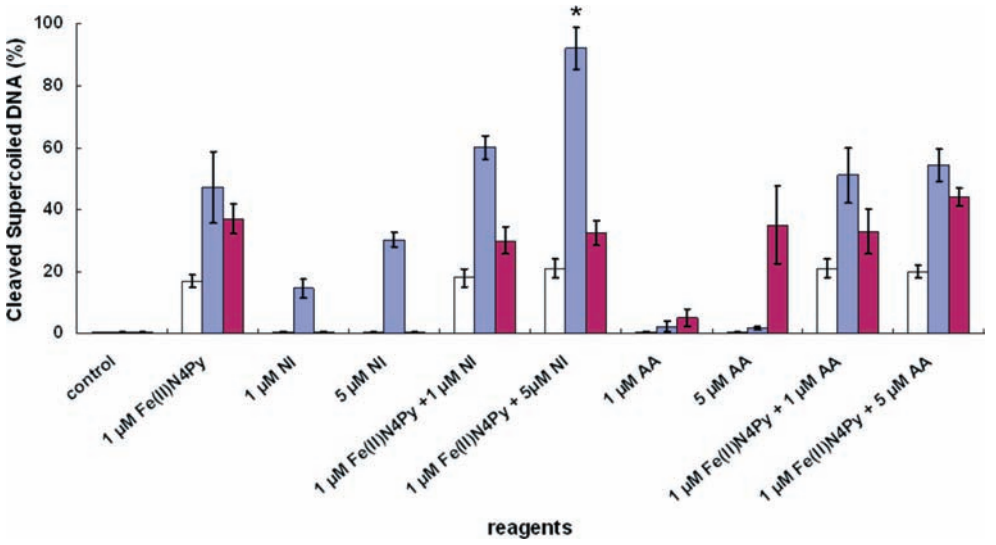

Figure 2. DNA cleavage at 30 min under ambient lighting (white bars), photo irradiation at 355 nm (2.6 mW) (blue bars), and 400.8 nm (1.2 mW) (purple bars). *Linear DNA was also formed.

RESULTS AND DISCUSSION

On the basis of the UV−vis absorption spectra of Fe(II)N4Py, NI, and AA (Figure 1), the wavelengths 355 and 400.8 nm were selected for photo irradiation in the DNA cleavage studies. In aqueous solution, the acetonitrile ligand of $[Fe(II)(N4Py)(CH_3CN)](ClO_4)_2 \cdot 2H_2O$ is displaced by a water molecule. This is demonstrated by ^1H NMR studies[5b] and cyclic voltammetry, which shows a shift of the oxidation potential from 1010 mV in acetonitrile[5c] to 50 mV vs SCE in aqueous solution (Figure S7, Supporting Information). From both UV−vis spectroscopy and cyclic voltammetry (Figures S5 and S6, Supporting Information) it is apparent that adduct formation between Fe(II)N4Py and NI or AA or other additives such as Tris buffer, dimethyl sulfoxide (DMSO), or NaN_3 does not occur.

DNA Cleavage. The DNA cleavage activities of the individual components, i.e., Fe(II)N4Py, NI, and AA, as well as the combination of Fe(II)N4Py with either NI or AA were investigated in the cleavage of supercoiled pUC18 (0.1 $\mu g\ \mu L^{-1}$, 150 μM bp) in 10 mM Tris-HCl buffer (pH of 8.0) at 37 °C in the absence of reducing agent over 30 min under laser irradiation at 355 (2.6) and 400.8 nm (1.2 mW), respectively. All of the experiments were carried out at least in triplicate independently.

Figure 2 and Table S1, Supporting Information, compare the DNA cleavage induced by 1 μM of Fe(II)N4Py and the combination of 1 μM of Fe(II)N4Py and 1 or 5 equiv of NI or AA under ambient lighting and with irradiation at 355 and 400.8 nm, by indicating the amounts of cleaved supercoiled DNA after 30 min.[10]

DNA Cleavage Efficiency of Fe(II)N4Py, NI, and AA. In the control experiment, i.e., in the absence of Fe(II)N4Py and chromophores, DNA cleavage was not observed under either ambient lighting or photo irradiation. One μM Fe(II)N4Py induced significant amounts of supercoiled DNA cleavage under irradiation at both 355 (47 ± 12%) and 400.8 nm (37 ± 5% conversion). More efficient DNA cleavage is observed with irradiation than under ambient lighting conditions (17 ± 2% conversion), consistent with our previous report.[5g]

Under ambient lighting conditions, both NI and AA did not cause DNA cleavage within 30 min. At 355 nm, where NI has a strong absorption at 355 nm ($\varepsilon = 1.16 \times 10^4\ M^{-1}\ cm^{-1}$), 15 ± 3% of substrate supercoiled DNA was cleaved by 1 μM of NI, which was increased to 30 ± 2% with 5 μM of NI. Under irradiation at 400.8 nm, where NI does not absorb, DNA cleavage was not observed with NI only.

With AA, which has only a weak absorption at 355 nm ($\varepsilon = 0.18 \times 10^4\ M^{-1}\ cm^{-1}$), less than 2% of DNA cleavage was observed with irradiation at 355 nm. At 400.8 nm, where AA has a moderate absorption ($\varepsilon = 0.92 \times 10^4\ M^{-1}\ cm^{-1}$), 5 ± 3% of supercoiled DNA was cleaved with 1 μM of AA, which increased to 35 ± 13% at 5 μM concentration.

DNA Cleavage Efficiency of Fe(II)N4Py Combined with NI. Under ambient lighting, comparable amounts of supercoiled DNA were cleaved by 1 μM Fe(II)N4Py alone and 1 μM Fe(II)N4Py combined with 1 and 5 equiv of NI as well as under photo irradiation at 400.8 nm (Figure 2). At 355 nm (Figure 2), 1 μM Fe(II)N4Py with 1 equiv of NI induced the cleavage of 60 ± 4% supercoiled DNA within 30 min, which is in the range of that observed without NI (47 ± 12%) within experimental uncertainty. Combined with 5 equiv of NI, a higher DNA cleavage efficiency was observed for 1 μM of Fe(II)N4Py: 92 ± 7% of supercoiled DNA was cleaved, which is the sum of the DNA cleavage efficiency of 1 μM of Fe(II)N4Py (60 ± 4%) and 5 μM of NI (30 ± 2%). However, in contrast to the cases with Fe(II)N4Py or NI alone, 12% of linear DNA was also formed. The linear DNA may be produced by both single- and double-strand DNA cleavage processes.[8] Statistical analysis indicates that 0.13 double-strand cuts (m) occurred for every 2.5 single-strand cuts (n) on one DNA molecule (Figure S3, Supporting Information), which is significantly larger than the theoretical value of $m = 0.019$ for a pure single-strand DNA cleavage process, as calculated from the Freifelder−Trumbo relationship.[9] Thus, at 355 nm direct double-strand DNA cleavage took place also in addition to single-strand DNA cleavage. Combined this indicates that at this wavelength, there is a substantial synergistic effect of Fe(II)N4Py and 5 equiv of NI. In contrast, at 400.8 nm no

dx.doi.org/10.1021/ic2008478 |Inorg. Chem. 2011, 50, 8318–8325

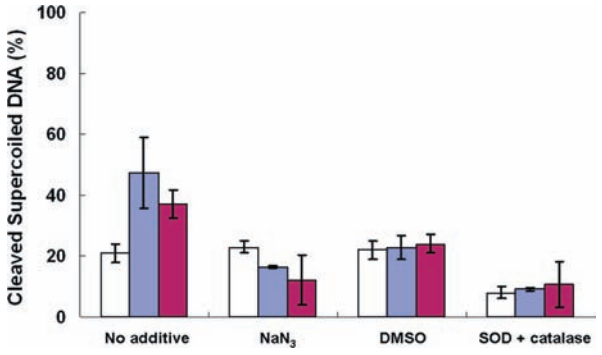

Figure 3. DNA cleavage at 30 min by 1 μM Fe(II)N4Py under ambient lighting (white bars), photo irradiation at 355 nm (2.6 mW) (blue bars), and 400.8 nm (1.2 mW) (purple bars).

significant synergistic effect was observed from the combination of Fe(II)N4Py and NI.

DNA Cleavage Efficiency of Fe(II)N4Py Combined with AA. Under both ambient lighting and irradiation at 355 and 400.8 nm, 1 μM Fe(II)N4Py alone and 1 μM Fe(II)N4Py combined with 1 and 5 equiv of AA induced comparable amounts of DNA cleavage. Thus the presence of AA did not influence the observed DNA cleavage efficiency of 1 μM of Fe(II)N4Py under these conditions.

ROS Involved in DNA Cleavage. A series of mechanistic probes was employed, including NaN_3, which is a known singlet oxygen ($^1O_2$) scavenger,[11] DMSO,[12] which acts as a hydroxyl radical ($HO^\bullet$) scavenger, a combination of SOD, which disproportionates superoxide radicals ($O_2^{\bullet-}$) into O_2 and H_2O_2,[13] and catalase, which disproportionates H_2O_2 into O_2 and H_2O,[14] to investigate the ROS involved in the DNA cleavage process. Addition of DMSO or NaN_3 does not result in a change in the redox properties of Fe(II)N4Py or Fe(III)N4Py, which indicates that they do not displace the bound water ligand (Figure S6a and b, Supporting Information). The effect of scavengers on the fraction of cleaved supercoiled DNA (%) is shown in Figures 3−6.

Effect of ROS Scavengers on DNA Cleavage with Fe(II)N4Py. As reported previously, in the absence of photo irradiation, NaN_3 and DMSO did not affect the DNA cleavage efficiency of Fe(II)N4Py, while SOD combined with catalase showed substantial inhibition (Figure 3). This indicates that $^1O_2$ and $HO^\bullet$ do not play an important role in DNA cleavage, while $O_2^{\bullet-}$ is a major contributor.[5g] Under photo irradiation, all three scavengers inhibited the DNA cleavage activity of Fe(II)N4Py alone (Figure 3), as indicated by the smaller amounts of supercoiled DNA cleaved, suggesting that $^1O_2$, $O_2^{\bullet-}$, and $HO^\bullet$ contribute to the DNA cleavage observed.[5g]

Effect of ROS Scavengers on DNA Cleavage with NI and AA. Five μM NI in combination with the mechanistic probes did not induce DNA cleavage under ambient lighting and photo irradiation at 400.8 nm (Figure 4a). At 355 nm, 5 μM of NI induced 30 ± 2% DNA cleavage within 30 min, which was not significantly altered by addition of either NaN_3 or DMSO. In contrast, SOD combined with catalase increased the DNA cleavage efficiency of NI substantially, with >60% of substrate supercoiled DNA being cleaved (Figure 4a), indicating that scavenging of $O_2^{\bullet-}$ and H_2O_2 has a significant enhancing effect on DNA cleavage. It has been reported that radicals derived from quenching of the triplet state of NI derivatives (^{3}NI*) by ground-state chromophores are more effective in cleaving DNA than reactive oxygen

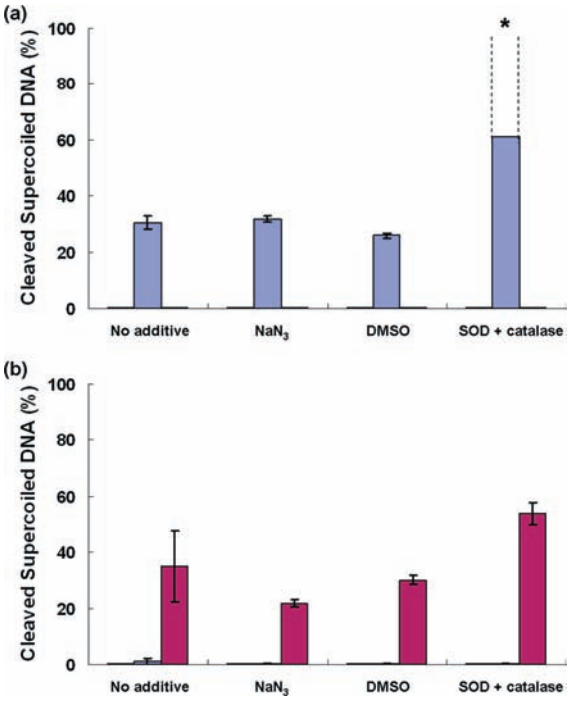

Figure 4. DNA cleavage at 30 min under ambient lighting (white bars), under photo irradiation at 355 nm (2.6 mW) (blue bars), and 400.8 nm (1.2 mW) (purple bars) by (a) 5 μM NI and (b) 5 μM AA. *Accurate quantification was not possible because of extensive DNA strand cleavage resulting in smearing on the gel. Therefore, the solid bar represents the lower limit of DNA cleavage.

species, albeit that this is proposed to proceed mainly via nucleobase oxidation.[15] Without scavengers, $O_2^{\bullet-}$ may quench ^{3}NI*. By scavenging $O_2^{\bullet-}$, more ^{3}NI* would be available in the solution for reaction with DNA. This would explain the significant increase in DNA cleavage achieved by adding SOD and catalase.

In the presence of 5 μM of AA, DNA cleavage was not observed at 30 min under ambient lighting and irradiation at 355 nm with any of the three ROS scavengers (Figure 4b). At 400.8 nm, 5 μM of AA alone induced 35 ± 13% DNA cleavage, whereas 22 ± 1 and 30 ± 2% DNA cleavage was observed by adding NaN_3 and DMSO, respectively (Figure 4b), indicating the quenching of $^1O_2$ and $HO^\bullet$ are not of significant importance in DNA cleavage by AA. By adding SOD and catalase, 5 μM of AA induced slightly more DNA cleavage (54 ± 4%) (Figure 4b).

Effect of ROS Scavengers on DNA Cleavage with Fe(II)N4Py/NI. As indicated above, 1 μM of Fe(II)N4Py with 5 μM of NI together induced the formation of linear DNA under photo irradiation at 355 nm within 30 min. To allow for comparison, in addition to the amounts of cleaved supercoiled DNA (Figure 5a), the amounts of linear DNA (Figure 5b) and the calculated values of single- (n) and double-strand cuts (m) per DNA molecule (Figure 5c) are shown also.

Under ambient lighting, the presence of 5 equiv of NI did not affect the DNA cleavage efficiency of 1 μM if Fe(II)N4Py (Figure 2). As expected, the same patterns of inhibition of ROS scavengers were observed for Fe(II)N4Py/NI and Fe(II)N4Py (Figures 5a and 3), i.e., NaN_3 and DMSO did not affect DNA cleavage efficiency, while SOD combined with catalase showed strong inhibitory effect.

At 355 nm, where the presence of 5 μM of NI increased the DNA cleavage efficiency of Fe(II)N4Py, NaN_3 did not inhibit

dx.doi.org/10.1021/ic2008478 |*Inorg. Chem.* 2011, 50, 8318–8325

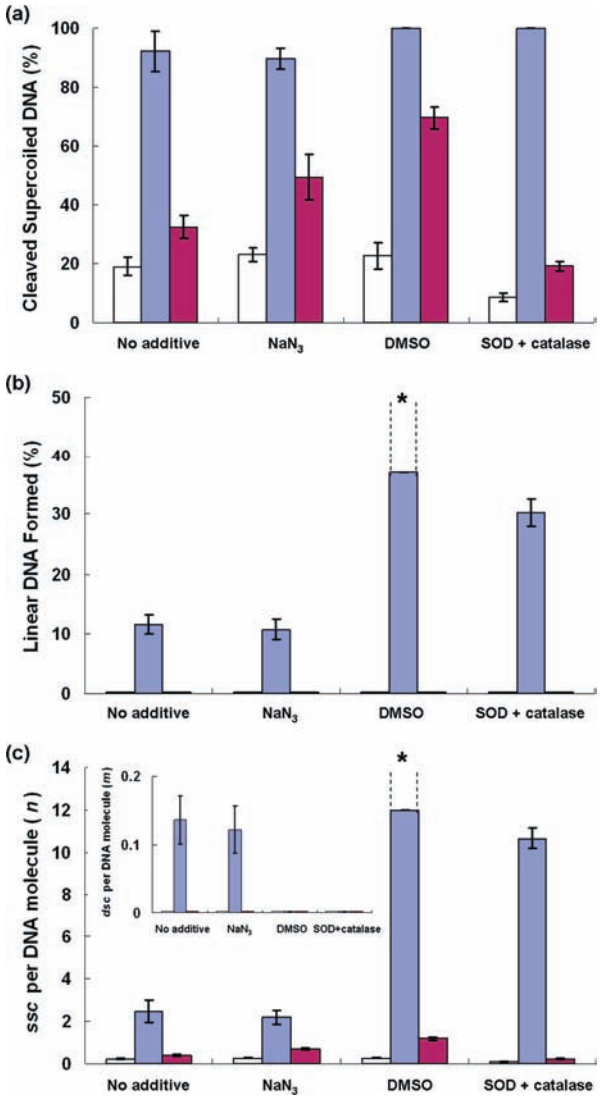

Figure 5. Under ambient lighting (white bars), photo irradiation at 355 nm (2.6 mW) (blue bars), and 400.8 nm (1.2 mW) (purple bars) for 1 μM of Fe(II)N4Py + 5 μM of NI at 30 min: (a) amounts of cleaved supercoiled DNA; (b) amounts of formed linear DNA; (c) the calculated average numbers of single-strand cuts per DNA molecule (n) for DNA cleavage; and insert: the calculated average numbers of double-strand cuts (m) per DNA molecule. *More than 37% of linear DNA was formed, which exceeded the limit of accurate quantification.[5d] Presented in (b) is the highest detectable amounts of linear DNA (37%), which represents the lower limit of the amount of linear DNA formed, and the solid bar presented in (c) is the lower limit of the calculated value of n.

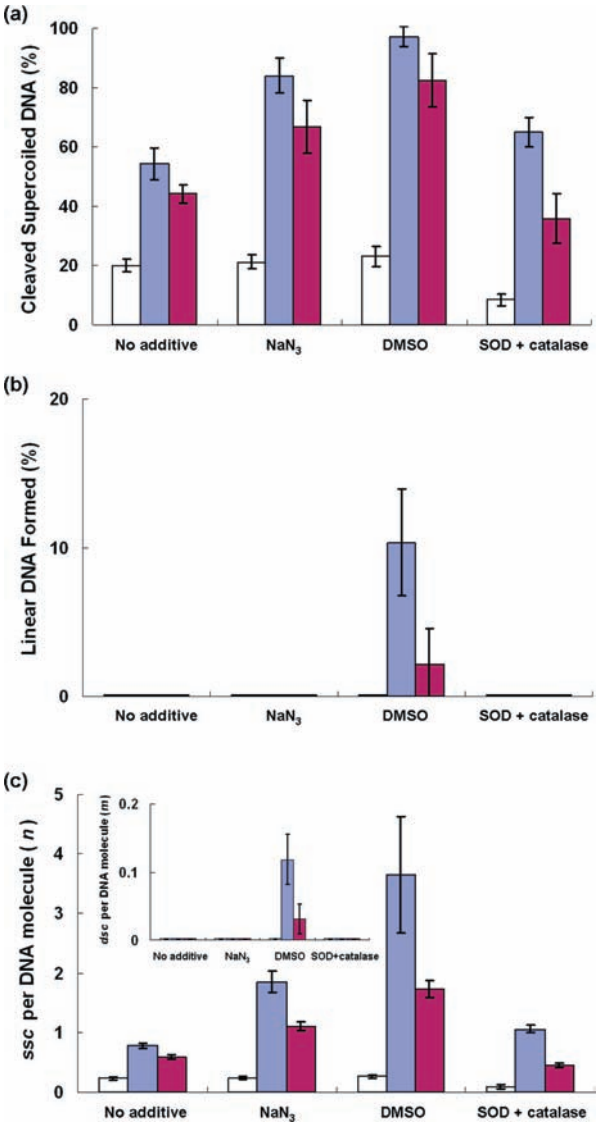

Figure 6. Under ambient lighting (white bars), photo irradiation at 355 nm (2.6 mW) (blue bars), and 400.8 nm (1.2 mW) (purple bars) for 1 μM of Fe(II)N4Py plus 5 μM AA at 30 min: (a) amounts of cleaved supercoiled DNA; (b) amounts of formed linear DNA; (c) the calculated average numbers of single-strand cuts per DNA molecule (n) for DNA cleavage; and insert: the calculated average numbers of double-strand cuts (m) per DNA molecule.

DNA cleavage by Fe(II)N4Py/NI: 90 $\pm$ 4% supercoiled DNA cleavage and a m of 0.12 $\pm$ 0.04 (Figure S3, Supporting Information) was found in the presence of NaN_3, compared to 92 $\pm$ 6% (Figure 5) and a m value of 0.14 $\pm$ 0.04 in the absence of NaN_3 (Figure S3, Supporting Information, ■). This indicates that the quenching of $^1O_2$ did not affect the observed DNA cleavage efficiency of Fe(II)N4Py/NI (Figure 3).

Surprisingly, by adding DMSO or SOD plus catalase the observed DNA cleavage efficiency of Fe(II)N4Py/NI was significantly increased. With DMSO, 100% of supercoiled DNA was cleaved and more than 37% linear DNA was formed, which is beyond the limit of accurate quantification.[5d] Therefore, the numbers representing the lower limit of DNA cleavage efficiency are shown in Figure 5b and c. By adding SOD with catalase, the substrate supercoiled DNA was also consumed completely. As indicated in Figure 5c, SOD with catalase together promoted the DNA cleavage efficiency of Fe(II)N4Py/NI from n = 2.5 $\pm$ 0.5 to 10.7 $\pm$ 0.5. A notable observation is that upon addition of DMSO or SOD plus catalase, the formation of linear DNA was inhibited completely, i.e., scavenging of $HO^\bullet$ or $O_2^{\bullet-}$ and H_2O_2 results in a substantial reduction in the double-strand cleavage activity.

At 400.8 nm a somewhat different pattern was observed. The presence of 5 equiv of NI did not affect the observed DNA cleavage activity of 1 μM of Fe(II)N4Py (Figure 2). By adding NaN_3 and DMSO, the conversion of supercoiled DNA by Fe(II)N4Py/NI was increased from 33 $\pm$ 4 to 50 $\pm$ 8 and

dx.doi.org/10.1021/ic2008478 |*Inorg. Chem.* 2011, 50, 8318–8325

70 ± 4% (Figure 5a), respectively. However, SOD together with catalase inhibited DNA cleavage, i.e., only 19 ± 2% cleavage of supercoiled DNA was found (Figure 5a), which is in contrast to that observed at 355 nm.

Effect of ROS Scavengers on DNA Cleavage with Fe(II)N4Py/AA. Under ambient lighting as well as under photo irradiation at 355 or 400.8 nm, 1 μM of Fe(II)N4Py combined with 5 μM of AA showed comparable DNA cleavage efficiency compared to 1 μM of Fe(II)N4Py alone (Figure 2). Without irradiation, as expected, the same patterns of inhibition by ROS scavengers were observed for Fe(II)N4Py/AA and Fe(II)N4Py alone (Figures 6a and 3), i.e., quenching of $^1O_2$ and $HO^\bullet$ did not affect DNA cleavage, and quenching of $O_2^{\bullet-}$ resulted in a significant decrease in DNA cleavage efficiency.

At 355 nm, by adding NaN_3 or DMSO, the observed DNA cleavage of Fe(II)N4Py/AA was increased from 54 ± 5 to 84 ± 6 and 97 ± 3%, respectively (Figure 6a). Moreover, in the presence of DMSO, 10 ± 4% linear DNA was formed (Figure 6b), which corresponds to a *m* of 0.12 compared to the *m* of 0.041 calculated based on the Freifelder−Trumbo relationship[9] (Figure 6c and Figure S4, Supporting Information), indicating that small amounts of double-strand cuts occurred also. By adding SOD with catalase, only a slightly higher DNA cleavage efficiency (65 ± 5%) was observed with Fe(II)N4Py/AA (Figure 6,). Thus, the quenching of $^1O_2$ and $HO^\bullet$ promotes the DNA cleavage activity of Fe(II)N4Py/AA, whereas quenching of $O_2^{\bullet-}$ has only a minor effect. A similar pattern was observed at 400.8 nm.

Origin of the Effect of ROS Scavenger on DNA Cleavage by Fe(II)N4Py/NI and Fe(II)N4Py/AA. Under ambient lighting, the same inhibition effect of ROS scavengers on DNA cleavage activity was observed for Fe(II)N4Py, Fe(II)N4Py/NI, and Fe(II)N4Py/AA (Figures 3, 5, and 6). This is not surprising since the chromophores are not excited, and hence PET cannot occur. Furthermore, this also suggests that the mechanism of oxygen activation by Fe(II)N4Py is not altered by the presence of NI or AA. However, when photo irradiation was employed, a very different and surprising effect was observed with ROS scavengers.

Under photo irradiation at 355 nm, by quenching $HO^\bullet$ and $O_2^{\bullet-}$, a dramatic increase in DNA cleavage activity was obtained with Fe(II)N4Py/NI, whereas no effect was observed by removing $^1O_2$ (Figure 5). To some extent, this is related to the increased activity observed for NI alone in the presence of SOD/catalase (vide supra). However, this is clearly only a part of the explanation in view of the very different pattern of activity observed upon the addition of scavengers. The results described here for the Fe(II)N4Py/NI system present a paradox: it has been well established that ROS, and in particular $O_2^{\bullet-}$, are key active species in Fe(II)N4Py-mediated DNA cleavage.[5f] Yet here it was observed that under irradiation and in the presence of NI and AA, actually the scavenging of these same reactive oxygen species gives rise to significantly higher DNA cleavage activity. The effect of the ROS scavengers in these reactions is highly surprising and at present not well understood. The complexity of the present system makes it difficult to unambiguously assign the origin of the observed effects and most likely a combination of factors contribute. However, based on the data available, a hypothesis can be presented to rationalize, at least partly, these unexpected effects of ROS scavengers.

First, we propose that the nature of the reactive species responsible for the enhanced DNA cleavage is not altered by the presence of NI. Thus, the origin of the enhancement in observed DNA cleavage activity is the increased rate of formation of N4Py-Fe(III)-OOH, due to the faster reduction of Fe(III), which is the species obtained after reaction of N4PyFe(II) with O_2 to produce $O_2^{\bullet-}$, aided by PET from the triplet excited state of NI (^{3}NI*) to Fe(III)N4Py (Scheme 1b).

Scheme 1. Possible Processes Involved in the ROS Scavenger-Enhanced DNA Cleavage with Fe(II)N4Py/NI under Photo Irradiation

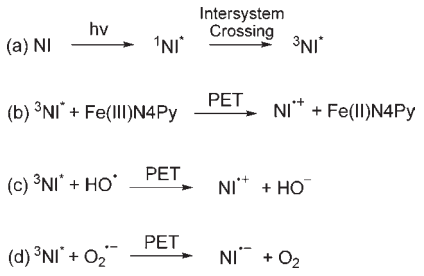

PET processes involving NI derivatives have attracted widespread attention because of the relatively long lifetime of the lowest triplet excited state.[16] The lifetime (τ_T) of ^{3}NI* in H_2O/CH_3CN (v/v = 1:1) has been determined to be in the range of 30−40 μs[17] and is expected to be similar in the buffered aqueous solutions employed in the present study. Therefore, τ_T of ^{3}NI* in the aqueous solutions used in the DNA cleavage reaction should be sufficiently long to allow for significant intermolecular electron-transfer processes to take place. As the reduction of Fe(III)N4Py back to Fe(II)N4Py has been shown to be rate limiting, the majority of the iron−N4Py complex present under reaction conditions will be in the Fe(III) redox state.[5f] The ΔG_{et} of PET from ^{3}NI* to Fe(III)N4Py under the conditions employed in the DNA cleavage studies is of the order of −7∼ −9 kcal mol^{-1} (see Supporting Information for details). Thus, the reduction of Fe(III) by ^{3}NI* will be thermodynamically favorable and contributes to the increased efficiency of DNA cleavage. However, a side reaction can also occur, which is the reaction of ^{3}NI* with $HO^\bullet$ and $O_2^{\bullet-}$ (Scheme 1c and d). As a result of this, the reduction of Fe(III) is not competitive, and thus no promoting effect of the chromophores on the DNA cleavage activity is observed. Therefore, the addition of scavengers, such as DMSO and SOD/catalase that decrease the concentration of $HO^\bullet$ and $O_2^{\bullet-}$, increases the probability of PET from ^{3}NI* to Fe(III)N4Py and thus increases the rate of reduction of Fe(III) back to Fe(II). As a result, an increase in DNA cleavage activity is observed.

It is important to realize that Fe(II)N4Py requires ROS, e.g., $^1O_2$ and $O_2^{\bullet-}$, to form the reactive species for DNA cleavage. As a consequence, ROS cannot be scavenged completely since this would also reduce DNA cleavage activity, as was shown before.[5f] So, whereas on the one hand a high concentration of ROS increases the rate of formation of the active iron species, on the other hand it decreases the efficiency of PET, which has a negative effect on the rate of formation of the active iron species. Consequently, there is an optimum concentration of ROS to achieve the highest DNA cleavage activity. Thus, the role of the ROS scavengers is most likely to maintain a (near) optimal concentration of ROS, which explains their overall promoting effect on DNA cleavage activity in the present system under irradiation.

Most likely similar effects as described for Fe(II)N4Py/NI at 355 nm are involved with AA and/or irradiation at 400.8 nm. However, the system is quite complex, comprising of multiple interacting components that respond differently to a change in the system. This may give rise to a change in the composition and nature of the ROS that are produced, which results in a different scavenger pattern. Indeed, we have shown before that in the absence of NI or AA, different ROS are produced depending on the wavelength of irradiation.[5g]

Also in the present system a wavelength dependence was observed. At 400.8 nm, the observed DNA cleavage activity of Fe(II)N4Py/NI was increased by quenching $^1O_2$ and $HO^\bullet$, whereas by scavenging $O_2^{\bullet-}$ it was decreased (Figure 5), which is a different pattern than observed at 355 nm. It is possible to generate ^{3}NI* by photo irradiation at 400.8 nm, even though NI does not show strong absorption at this wavelength (Figure 1), albeit that much smaller amounts of ^{3}NI* will be formed. This would account for the less significant effect of scavenging $HO^\bullet$ and $O_2^{\bullet-}$, compared to that observed at 355 nm.

Replacing NI with AA resulted in a different scavenger pattern compared to Fe(II)N4Py/NI. A notable change is that in addition to $HO^\bullet$ and O_2, quenching of $^1O_2$ also resulted in increased DNA cleavage activity, albeit that in general the effects were substantially less pronounced (Figure 6). The efficiency of reduction of Fe(III)N4Py by the triplet state of AA (^{3}AA*) is significantly reduced due to the short lifetime (τ_T) of ^{3}AA* in H_2O, which has been determined to be in the range of 15−20 ns.[18] Moreover, the relative weaker absorption of AA ($\varepsilon = 0.18 \times 10^4\ M^{-1}\ cm^{-1}$) compared to NI ($\varepsilon = 1.16 \times 10^4\ M^{-1}\ cm^{-1}$) at 355 nm is also likely to contribute to the less significant effect of ROS scavengers.

CONCLUSIONS

The present study compared the DNA cleavage efficiency of Fe(II)N4Py alone, Fe(II)N4Py combined with NI, and Fe(II)N4Py combined with AA under ambient lighting and photo irradiation at 355 and 400.8 nm under aerobic conditions. Under photo irradiation at 355 nm, the DNA cleavage efficiency of Fe(II)N4Py was increased significantly in the presence of 5 equiv of NI, indicating a synergestic effect, whereas at 400.8 nm or with AA no beneficial effect was observed. Surprisingly in many cases the addition of ROS scavengers gave rise to substantially increased DNA cleavage activity. Most likely, the ROS scavengers ensure a concentration of the ROS that give rise to the optimal balance between PET from the chromophores to the Fe(III)N4Py complex, resulting in the reduction to the Fe(II) state and the formation of the active iron complexes by reaction of the Fe(II) complex with ROS, that are responsible for DNA cleavage. Importantly, these results clearly illustrate the care that should be exercised in the analysis of data resulting from the addition of ROS scavengers as they can give rise to very unexpected results, especially if the complexity of the system is increased, that are not easily interpreted in terms of a single simplified mechanism.

ASSOCIATED CONTENT

Supporting Information. Experimental setup; determination of irradiation power; supporting table of DNA cleavage data; graphs of double-strand (m) over single-strand cuts (n) as evidence for direct double-strand DNA cleavage; UV−vis absorption spectra of Fe(II)N4Py in the presence of NI and AA; cyclic voltammetry of Fe(II)N4Py in the absence and presence of DMSO, NaN_3, NI, and AA; and estimation of ΔG_{et} for PET of ^{3}NI*/Fe(III)N4Py. This material is available free of charge via the Internet at http://pubs.acs.org.

AUTHOR INFORMATION

Corresponding Authors

*E-mail: w.r.browne@rug.nl, j.g.roelfes@rug.nl.

ACKNOWLEDGMENT

Financial support from the University of Groningen, NRSC-Catalysis, and Netherlands Organization for Scientific Research (NWO) is gratefully acknowledged.

REFERENCES

(1) Umezawa, H.; Maeda, K.; Takeuchi, T.; Okami, Y. *J. Antibiot.* **1966**, *19*, 200–209.

(2) Hecht, S. M. *Bleomycin: Chemical, Biochemical and Biological Aspects*; Springer: New York, 1979.

(3) (a) Burger, R. M. *Chem. Rev.* **1998**, *98*, 1153–1170. (b) Claussen, C. A.; Long, E. C. *Chem. Rev.* **1999**, *99*, 2797–2816.

(4) Hecht, S. M. *J. Nat. Prod.* **2000**, *63*, 158–168.

(5) (a) Lubben, M.; Meetsma, A.; Wilkinson, E. C.; Feringa, B. L.; Que, L., Jr. *Angew. Chem., Int. Ed. Engl.* **1995**, *34*, 1512–1514. (b) Roelfes, G.; Branum, M. E.; Wang, L.; Que, L., Jr.; Feringa, B. L. *J. Am. Chem. Soc.* **2000**, *122*, 11517–11518. (c) Roelfes, G.; Vrajmasu, V.; Chen, K.; Ho, R. Y. N.; Rohde, J.; Zondervan, C.; la Crois, R. M.; Schudde, E. P.; Lutz, M.; Spek, A. L.; Hage, R.; Feringa, B. L.; Münck, E.; Que, L., Jr. *Inorg. Chem.* **2003**, *42*, 2639–2653. (d) van den Berg, T. A.; Feringa, B. L.; Roelfes, G. *Chem. Commun.* **2007**, 180–182. (e) Megens, R. P.; van den Berg, T. A.; de Bruijn, A. D.; Feringa, B. L.; Roelfes, G. *Chem.—Eur. J.* **2009**, *15*, 1723–1733. (f) Li, Q.; van den Berg, T. A.; Feringa, B. L.; Roelfes, G. *Dalton Trans.* **2010**, 8012–8021. (g) Li, Q.; Browne, W. R.; Roelfes, G. *Inorg. Chem.* **2010**, *49*, 11009–11017.

(6) For examples, see: (a) Buchardt, O.; Egholm, M.; Karup, G.; Nielsen, P. E. *J. Chem. Soc., Chem. Commun.* **1987**, 1696–1697. (b) Nielsen, P. E.; Jeppesen, C.; Egholm, M.; Buchardt, O. *Nucleic Acids Res.* **1988**, *16*, 3877–3888. (c) Saito, I.; Takayama, M.; Kawanishi, S. *J. Am. Chem. Soc.* **1995**, *117*, 5590–5591. (d) Aveline, B. M.; Matsugo, S.; Redmond, R. W. *J. Am. Chem. Soc.* **1997**, *119*, 11785–11795. (e) Da Ros, T.; Spalluto, G.; Boutorine, A. S.; Bensasson, R. V.; Prato, M. *Curr. Pharm. Des.* **2001**, *7*, 1781–1821. (f) Joseph, J.; Eldho, N. V.; Ramaiah, D. *Chem.—Eur. J.* **2003**, *9*, 5926–5935. (h) Xu, Y.; Huang, X.; Qian, X.; Yao, W. *Bioorg. Med. Chem.* **2004**, *12*, 2335–2341. (g) Fernández, M.-J.; Wilson, B.; Palacios, M.; Rodrigo, M.-M.; Grant, K. B; Lorente, A. *Bioconjugate Chem.* **2007**, *18*, 121–129.

(7) Montalti, M.; Credi, A.; Prodi, L.; Gandolfi, M. T. *Handbook of Photochemistry*, 3rd ed.; CRC Press: Boca Raton, FL, 2006.

(8) (a) Cowan, R.; Collis, C. M.; Grigg, G. W. *J. Theor. Biol.* **1987**, *127*, 229–243. (b) Povirk, L. F.; Wübker, W.; Köhnlein, W.; Hutchinson, F. *Nucleic Acids Res.* **1977**, *4*, 3573–3580.

(9) Freifelder, D.; Trumbo, B. *Biopolymers* **1969**, *7*, 681–693.

(10) Under ambient lighting, the observed DNA cleavage activity was comparable to experiments in the dark, within experimental error margin.

(11) Hasty, N.; Merkel, P. B.; Radlick, P.; Kearns, D. R. *Tetrahedron Lett.* **1972**, *1*, 49–52.

(12) Repine, J. E.; Pfenninger, O. W.; Talmage, D. W.; Berger, E. M.; Pettijohn, D. E. *Proc. Natl. Acad. Sci. U.S.A.* **1981**, *78*, 1001–1003.

(13) (a) McCord, J. M.; Fridovic, I. *J. Biol. Chem.* **1969**, *244*, 6049–6055. (b) Lah, M. S.; Dixon, M. M.; Pattridge, K. A.; Stallings, W. C.; Fee, J. A.; Ludwig, M. L. *Biochemistry* **1995**, *34*, 1646–1660. (c) Dismukes, G. C. *Chem. Rev.* **1996**, *96*, 2909–2926. (d) Vance, C. K.; Miller, A. F. *Biochemistry* **2001**, *40*, 13079–13087.

(14) Wu, A. J.; Penner-Hahn, J. E.; Pecoraro, V. L. *Chem. Rev.* **2004**, *104*, 903–938.

(15) (a) Rogers, J. E.; Abraham, B.; Rostkowski, A.; Kelly, L. A. *Photochem. Photobiol.* **2001**, *74*, 521–531. (b) Saito, I.; Takayama, M.; Sugiyama, H.; Nakantani, K. *J. Am. Chem. Soc.* **1995**, *117*, 6406–6407.

(16) For recent examples, see: (a) Duke, R. M.; Veale, E. B.; Pfeffer, F. M.; Kruger, P. E.; Gunnlaugsson, T. *Chem. Soc. Rev.* **2010**, *39*, 3936–3953. (b) Veale, E. B.; Gunnlaugsson, T. *J. Org. Chem.* **2010**, *75*, 5513–5525. (c) McAdam, C. J.; Robinson, B. H.; Simpson, J.; Tagg, T. *Organometallics* **2010**, *29*, 2474–2483. (d) Huang, J.; Xu, Y.; Qian, X. *Org. Biomol. Chem.* **2009**, *7*, 1299–1303. (e) Kucheryavy, P.; Li, G.; Vyas, S.; Hadad, C.; Glusac, K. D. *J. Phys. Chem. A* **2009**, *113*, 6453–6461. (f) Cho, D. W.; Fujitsuka, M.; Sugimoto, A.; Majima, T. *J. Phys. Chem. A* **2008**, *112*, 7208–7213. (g) Takahashi, S.; Nozaki, K.; Kozaki, M.; Suzuki, S.; Keyaki, K.; Ichimura, A.; Matsushita, T.; Okada, K. *J. Phys. Chem. A* **2008**, *112*, 2533–2542.

(17) Cho, D. W.; Fujitsuka, M.; Yoon, U. C.; Majima, T. *Phys. Chem. Chem. Phys.* **2008**, *10*, 4393–4399.

(18) Kasama, K.; Kikuchi, K.; YNishida, Y.; Kokubun, H. *J. Phys. Chem.* **1981**, *85*, 4148–4153.